Polymer Journal (2018) 50:511–521
https://doi.org/10.1038/s41428-018-0036-8

ORIGINAL ARTICLE

Tissue-engineered scaffold based on carboxymethyl chitin or chitosan for corneal epithelial transplantation

Tong Li[1] · Ye Liang[2] · Zheying Wang[1] · Wenhua Zhang[1] · Liping Wang[2] · Quan Zhou[3] · Wenhua Xu[1]

Received: 15 August 2017 / Revised: 2 December 2017 / Accepted: 13 February 2018 / Published online: 16 March 2018

Abstract

Blend membranes based on polysaccharides are used in tissue engineering. In this study, six groups of blend membranes were prepared with carboxymethyl chitosan (CMCTS) or carboxymethyl chitin (CMCT) as the main ingredient, blended with gelatin (Gel) and potassium acetate (KAc). Then, each group was screened and evaluated for light transmission, microstructure, and compatibility with corneal epithelial cells. The results showed that the CMCTS-Gel blend membrane (#1) and the CMCT-Gel blend membrane (#4) (volume ratio of 20:1), which had high transmittance and good surface properties, were more suitable for cell growth. Although the primary corneal epithelial cells (CECs) seeded on both blend membranes maintained marker protein expression and did not undergo cell fibrosis, the CECs on the CMCT-Gel blend membrane (#4) maintained the original epithelial morphology and showed substantially improved K12 protein levels. Studies on the potential mechanism of the anti-fibrosis effect also showed that both membranes could block the phosphorylation of Smad2 and Smad3. In addition, the CMCT-Gel blend membrane (#4) could depress the total expression of native Smad2 and Smad3.This study provides a potential corneal epithelial scaffold that will be applied in corneal epithelial reconstruction based on tissue engineering methods.

Introduction

In 2010, the World Health Organization released the latest data, revealing that the number of blind people in China was approximately 8.25 million. Corneal disease was the second highest cause of blindness in China, accounting for 15.4% of cases. Surveys from various regions showed that more than half of the cases of blindness and visual impairment can be prevented or treated [1]. Corneal transplantation is an effective therapy for corneal blindness. However, there are still many limitations including the source, the preservation of donor cornea, postoperative graft rejection, and others, which makes further research on artificial corneas a topic of great interest in the field of tissue engineering.

Chitin (CT) is a natural polysaccharide with a positive charge. Chitosan (CTS), the *N*-deacetylated derivative of CT, has been widely used in the medical field [2–6]. Materials based on CTS have generally been used as cell scaffolds in various tissues or organs such as the bone, cartilage, intestine, peripheral nerve, and heart [7–11]. However, the applications of CTS and CT are highly restricted because of their poor solubility [12]. However, CTS and CT contain different groups that can be chemically modified, and carboxymethyl chitosan (CMCTS) and carboxymethyl chitin (CMCT) are among the most important water-soluble derivates and have been widely used in biomedical fields as drug carriers, antimicrobial materials, and tissue engineering materials because of their relatively toxicity and good biocompatibility [13]. To prepare materials that could be more suitable for cellular adherence and cell growth in corneal tissue engineering, different concentration of porogens and crosslinking agents should be considered. Potassium acetate has been applied in the field of biomaterials as a porogen [14, 15] because it can change

These authors contributed equally: Tong Li, Ye Liang.

✉ Wenhua Xu
qd.wh@163.com

[1] Department of Inspection, Qingdao University, Qingdao 266003, China

[2] Department of Urology and Andrology, Key Laboratory, Qingdao 266003, China

[3] Central Laboratory, Affiliated Hospital of Qingdao University, Qingdao 266003, China

the microstructure of materials by varying the diameters of holes and the spacing between them.

In addition, a number of studies have shown that CT, CTS, and its derivatives have an inhibitory effect on fibrous adhesion or scarring. This effect can be detected in the abdominal wall, eye, and tendon, in epidural scar formation and in other tissues and organs [16–19]. Thus, materials based on CTS or CT may play an important role in preventing fibrosis in corneal epithelia reconstruction. However, the effects of a scaffold based on CMCTS or CMCT have not been evaluated.

Corneal wound healing reactivity is a process that often leads to corneal scarring. Transforming growth factor-beta (TGF-β) is perhaps the key cytokine in the pathogenesis of cornea fibrotic disease [20]. If the TGF-β level rises substantially after injury, a fibrous scar will be formed easily, and the transparency of the cornea will be severely affected [21]. Therefore, we preliminarily investigated the effects of CMCTS or CMCT blend membranes on the TGF-β signaling pathway when the fibrosis of corneal epithelial cells was induced by TGF-β.

In this study, we used CMCTS or CMCT as the main ingredient to prepare blend membranes with good light transmittance, surface properties, and cell compatibility. Primary corneal epithelial cells cultured on these blend membranes were able to maintain the original morphology and the presence of marker proteins. The membranes were able to prevent cell fibrosis by regulating the total levels or the phosphorylation levels of the Smad2 and Smad3 proteins induced by TGF-β and therefore could potentially serve as scaffolds for corneal epithelial reconstruction.

Materials and methods

Materials and reagents

CMCTS and CMCT were prepared in our laboratory [22, 23]. Gel, 3-(4,5-dimethylthiazol-2-yl)-2,5-diphenyltetrazolium bromide (MTT) and 1,4-butanediol diglycidyl ether (BDDGE) were purchased from Sigma Chemical Co. (St. Louis, MO, USA). Materials for cell culture, including 1640 culture medium, fetal bovine serum (FBS), trypsin, penicillin and streptomycin, were purchased from Gibco Co. (Grand Island, NY, USA).The human corneal epithelial cell line (HCE) was procured from ATCC. The Agriculture Science Research Department of Shandong Province provided us with rabbits, and all procedures involving rabbits were performed in accordance with the ARVO Statement for the Use of Animals in Ophthalmic and Vision Research.

Table 1 Formulas of the six groups of blend membranes

Membrane	Components	Ratio of the components
#1	CMCTS-Gel	20:1
#2	CMCTS-Gel-KAc	20:1:5
#3	CMCTS-Gel-KAc	20:1:10
#4	CMCT-Gel	20:1
#5	CMCT-Gel-KAc	20:1:5
#6	CMCT-Gel-KAc	20:1:10

Preparation of CMCTS and CMCT blend membranes

First, a 2% CMCTS or CMCT solution was mixed with 2% Gel and different ratios of potassium acetate (KAc). Then, 5% BDDGE ethanol solution was added to the mixtures (at a volume ratio of 200:1) as crosslinker. After adequate stirring, the mixtures were poured into flat-bottomed dishes and dried at 30 °C to form thin membranes, which were numbered from #1 to #6 (Table 1). Then, the CMCTS or CMCT blend membranes were soaked with double-distilled water and drilled with a puncher to obtain diameters of 6 or 11 mm.

Transparency and surface microstructure of the blend membranes

The transparency was examined by penetrating the membranes with different wavelengths (400,500, 600, 700, 800 nm)of light and zeroing with distilled water(Thermo Multiskan Go Spectrum, Finland). The surface microstructure of the blend membranes was detected by a scanning electron microscope (SEM) (JEOL JSM-840, Japan). Six groups of membranes were preserved separately in normal saline. Then, the membranes were dried with a critical point dryer, sputter-coated with gold in a high-vacuum evaporator and visualized by SEM.

Evaluation of cytocompatibility with HCE cells

Sterile blend membranes (11 mm in diameter) were first placed in 48-well tissue culture plates in advance. Then, HCE cells were seeded on the membranes at a density of 5×10^5 cells/ml. Wells without membranes but otherwise treated the same were used as controls. All the wells were cultured at 37 °C/5% CO_2 with the medium changed every 2 days. The adhesion and proliferation of the cells were monitored by light microscopy. On the 4th day, the cell growth was detected by the MTT assay. Medium without cells was used as a blank control. The relative growth rate (RGR, %) was calculated by the following formula: RGR $(\%) = (OD_1 - OD_0)/(OD_2 - OD_0) \times 100\%$. OD_0, OD_1, and OD_2 were the average OD values of the blank, experimental and control groups, respectively. Experiments were performed in sextuplicate.

Table 2 Properties of CMCTS and CMCT

Material	Molecular weight	Water content	Degree of deacetylation	Degree of carboxymethylation	Heavy metal content
CMCTS	134 kDa	18.23%	96.44%	103.64%	≤10 μg/g
CMCT	115 kDa	17.21%	40.5%	96.76%	≤10 μg/g

Primary corneal epithelial cells cultured on scaffolds

Primary corneal epithelial cells (CECs) were excised from the normal eyes of New Zealand white rabbits aged 2–3 months. The rabbit CECs were cultured with DMEM/F12 medium containing 15% FBS by the tissue block method. The cultured cells were then incubated at 37 °C/5% CO_2 for subsequent experiments. Cytocompatibility was also evaluated by culturing CECs on the screened membranes by the same method as in 2.4. CECs on blend membranes were incubated at 37 °C in 5% CO_2 for 48 h and then labeled with 5,6-carboxy fluorescein diacetate succinimidyl ester (CFSE).The adhesion and proliferation were observed by fluorescence microscope (CKX41SF, Olympus, Japan).

Markers of CECs identified by immunofluorescence and western blot assay

The preparation of stromal cells is similar to that of CECs. Stromal cells were also excised from the normal eyes of New Zealand white rabbits aged 2–3 months. The cornea is divided into three layers, the middle layer of which consists of stromal cells and the outermost layer of corneal epithelial cells. The middle layer of tissue was sheared and then cultured with a trypsin enzyme-digesting technique in vitro. Finally, the cells were cultured in DMEM/F12 medium containing only 10% FBS by the tissue block method. The cells were then incubated at 37 °C in 5% CO_2 for subsequent experiments.

CECs were cultured on the preliminarily screened membranes. In addition, cells were grown on glass slides as a control. After 4 days, the cells were rinsed with PBS, fixed in 4% paraformaldehyde at room temperature for 15 min and washed with PBS. The fixed cells were incubated in blocking buffer (5% BSA) at room temperature for 30 min, then with primary anti bodies against cytokeratin 3 + 12 (K3 + 12, Abcam, Cambridge, UK) and vimentin (Bioss, Beijing, China) diluted in the same blocking buffer at 4 °C overnight and with Cy3 or FITC-conjugated secondary antibodies for 1 h at room temperature. After rinsing with PBS, DAPI was used to stain the cell nuclei at room temperature for 10 min. The immunofluorescence slides were observed under a fluorescence microscope (CKX41SF, Olympus, Japan).

After CECs were cultured on screened membranes for 4d, the cell lysates were harvested for western blot analysis, which was performed according to a standard protocol. Mouse monoclonal anti-K3 + 12 antibody, rabbit polyclonal anti-vimentin antibody, and mouse monoclonal anti-GAPDH antibody (Novus, Colorado, USA) were used as the primary antibodies. Chemiluminescent substrate for HRP detection was purchased from Millipore (Bedford, MA, USA).An imaging system (Vilber Lourmat Fusion FX7, France) was used to image the protein bands. The data were normalized to GAPDH.

The potential mechanism by which blend membranes prevent epithelial cell fibrosis via the TGF-β pathway

Because of the limitations of anti-rabbit antibodies, HCE cells were used for the study of the mechanism. In the experimental groups, screened CMCTS and CMCT membranes were first placed into 48-well plates, and then cells were seeded at a density of 5×10^5 cells/ml. Cells cultured on the plate alone were used as normal controls. Half of each group was treated with TGF-β (10 ng/ml) for 1.5 h to induce cell fibrosis. The cell lysates of all groups were harvested for use in Western blot analysis. Antibodies against phospho-Smad2 (P-Smad2, Ser465/467), phospho-Smad3 (P-Smad3, Ser423/425), Smad2, and Smad3 were purchased from Cell Signaling Technology (CST, Denver, USA). An antibody against GAPDH was purchased from Sigma Chemical Co. (St. Louis, MO, USA). An imaging system (Vilber Lourmat Fusion FX7, France) was used to image the protein bands.

Statistical analysis

The data are shown as the mean ± SD (standard deviation) of a representative point from duplicated experiments. Statistical analysis of the data was performed by one-way analysis of variance or *t*-test, and a value of $P < 0.05$ was considered to reflect a significant difference (computed by SPSS version 19.0).

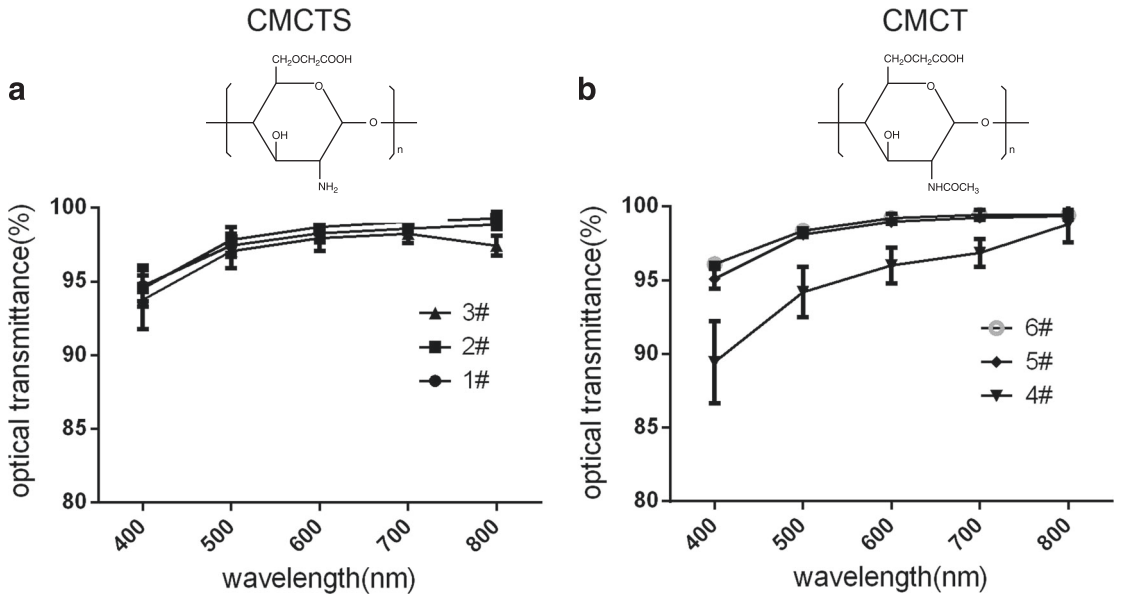

Fig. 1 Optical transmittance of membranes#1, #2, and #3 (**a**) and membranes #4, #5, and #6 (**b**) underlight wavelengths ranging from 400 to 800 nm. Each point represents the mean ± SD of three experiments

Results

Physicochemical properties and optical transmittance of the blend membranes

The materials CMCTS and CMCT, which were used to prepare the blend membranes as the scaffold of corneal transplantation, possess good water solubility, and their properties are presented in Table 2. The prepared CMCTS was measured to have a molecular weight of 134 kDa with 96.44% degree of deacetylation and 103.64% degree of carboxymethylation. And the prepared CMCT was determined to have a molecular weight of 115 kDa with 40.5% degree of deacetylation and 96.76% degree of carboxymethylation. The water content of CMCTS and CMCT was presented to be 18.23 and 17.21%, respectively. Heavy metal content was lower than 10 μg/g, which conforms to the national standards. We measured the optical transmittance for wavelengths ranging from 400 to 800 nm (Fig. 1a, b), as the transparency of the membrane is a critical indicator for a transplantation scaffold. The observed transmittance of all the membranes observed was almost uniformly greater than 90% under the tested visible wavelengths. The results indicated that the optical transmittance of these blend membranes could meet the requirements for corneal epithelial carriers. Previous studies have demonstrated that in certain spectral regions (at 450, 500, 550, 600, and 650 nm), the light transmission values of human corneas in the eye bank ranged from 50 to 75% [24]. According to these data, the blend membranes were obviously more transparent than human corneas.

The microstructure of the blend membranes

Surface properties are very important for evaluating potential scaffolds. The microstructure and roughness of the membranes will directly affect cell adhesion and growth. The microstructure of each blend membrane is shown in Fig. 2. Membranes #1, #2, and #3 are shown to have punctiform surfaces, and the porosity increases gradually with increasing porogen (KAc) content. On the other hand, blend membranes #4, #5, and #6 exhibit diagonal surface character. However, the surface of membrane #6, with the higher concentration of KAc, is much smoother than that of #4 and #5. Accordingly, the analysis of the surface properties of these membranes and the growth status of epithelial cells cultured on them will be described below.

Morphology and activity of HCE cells on the membranes

To investigate the cytocompatibility of the membranes, HCE cells were cultured on sterile blend membranes, and the cell status was observed by optical microscopy at 24 and 48 h (Figs. 3a, b). The results showed that cells on membranes #1 and #4 could reach almost complete confluence at 48 h, while cells on membrane #5 reached nearly 50% confluence, and membrane #2 and #3 barely showed adhering cells. However, some cells appeared on membrane #6 at 24 and 48 h, which might be related to its smoother microstructure, as mentioned above. On day 4, the cellular activity of each group was detected by MTT assay (Fig. 3c). The OD_{490} value of each experiment group was consistent

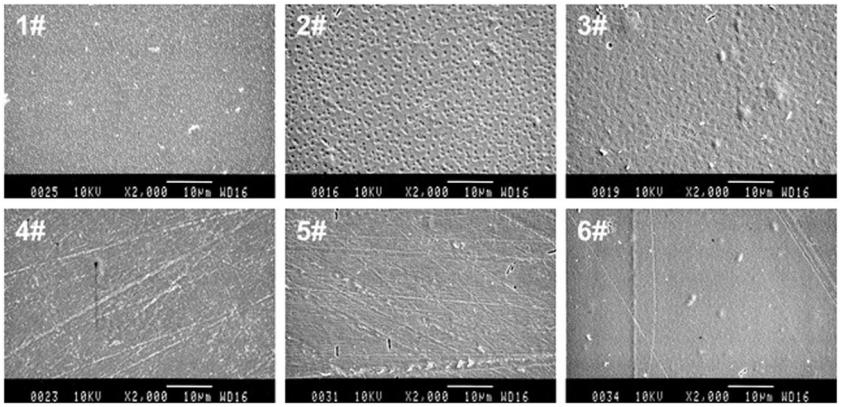

Fig. 2 Microstructure of the blend membranes observed by SEM. Membranes #1, #2, and #3 showed different degrees of punctiform structure, while blend membranes #4, #5, and #6 had diagonal surface character

with the respective micrographs. Thus, membranes #1 and #4 were screened in the subsequent studies.

Rabbit primary cells of corneal epithelia cultured on the screened membranes

The morphology of the primary CECs was observed by light microscopy, which emigrated from the tissue block after being cultured for 24 h and reached confluence after being cultured for 5 days (Fig. 4a). CECs were grown on the preliminarily screened membranes #4 and #1. After being cultured for 48 h, fluorescence microscope imaging at different magnification revealed the cell adhesion and morphology (Fig. 4b).There were more round cells on membrane #1, while the cells on membrane #4 could attach to each other and maintain the original epithelial morphology, in contrast to CECs cultured on glass slides as the control. These results showed that the membrane based on CMCT (#4) could be more suitable for culturing CECs than CMCTS (#1).

Effect of membranes on the marker protein expression of CECs, as shown by immunofluorescent observation

To further investigate the influence of the membranes on the CECs, immunofluorescent staining was carried out to detect the marker protein expression. Cytokeratin 3 and 12 (K3 + 12), which are specifically expressed in the corneal epithelia, are the typical marker proteins of CECs. In addition, vimentin is the marker protein of cells exhibiting, including stromal cells (SCs). Hence, vimentin staining (green) is used to indicate whether fibrosis is occurring in CECs cultured in vitro, and its expression in SCs serves as the positive control. Figure 5 shows that the CECs cultured on membrane #4, membrane #1 and glass slides (the control) all maintained K3 + 12 expression (red). However, green fluorescence could be detected in the control, and there was no vimentin staining for the CECs cultured on membranes #4 and #1. All these results indicated that the CECs could maintain marker protein expression and did not undergo cell fibrosis.

Detection of marker protein expression levels

Western plots were used to compare the expression levels of the epithelial marker K3 + 12 and the fibrosis marker vimentin in CECs grown on membranes #4 and #1 with the control cells cultured on glass plates (Fig. 6a). The data were normalized to GAPDH, and there were no significant changes in the K3 protein levels ($P > 0.05$) between the different groups of CECs (Fig. 6b). In addition, the K12 protein level in the cells grown on membrane #4 was substantially better than that of the control (Fig. 6c). The most important is the level of vimentin protein, which was expressed in the control, although it was much lower than in the positive control of SCs (Fig. 6d). However, vimentin was not detected in the two experimental groups (Fig. 6a). These results showed that the CECs cultured on the two membranes in vitro could maintain the native properties of the epithelia and did not undergo fibrosis when they were cultured, which was in accordance with the conclusions based on immunofluorescence.

Blend membranes suppressed epithelial fibrosis by regulating the TGF-β/Smad pathway

According to the results above, the CECs grown on membranes #4 and #1 maintainednormal epithelial morphology and K3 + 12 markers, and cell fibrosis could be prevented, which may be related to the role of the membranes. The potential mechanism was studied simultaneously. The expression data were normalized to GAPDH, and the phosphorylation of Smad2 and Smad3inducedby TGF-β were significantly reduced in epithelial cells cultured on membranes #4 and #1 in comparison with the group treated with TGF-β alone (Figs. 7a, b, d, e).There were no significant changes in the total Smad2 and Smad3incells

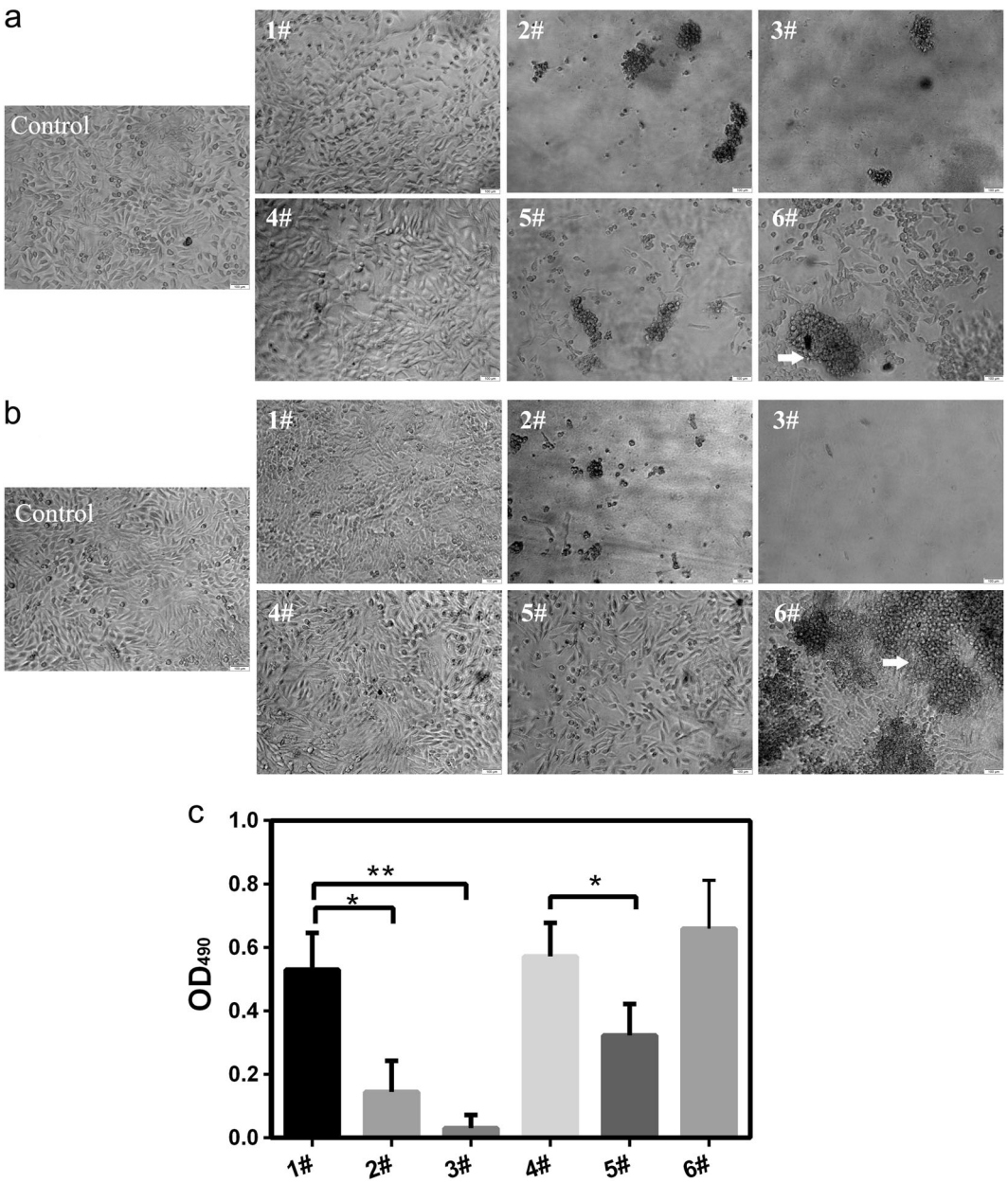

Fig. 3 The spread of the HCE cells on the six groups of blend membranes wasobserved by light microscopy after culturing for 24 h (**a**) and 48 h (**b**), and the arrows indicate that cells accumulatedon membrane #6 at both 24 and 48 h after cultivation. The OD 490 values at 96 h for HCE cells cultured on the blend membranes (**c**). Each result represents the mean ± SD of six experimental data points. $*p < 0.05$: significantly different; $**p < 0.01$: highly significantly different

cultured on membrane #1. However, for cells on membrane #4 without TGF-β induction, the total endogenous levels of Smad2 and Smad3 were significantly reduced (Figs. 7c, f).

Discussion

The corneal epithelia are located in the outermost layer of the cornea, which is easily injured. During wound healing, epithelial regeneration can be a critical factor in maintaining the transparency and function of the cornea. If the wound cannot be healed in time, the eyesight is affected, and corneal scarring occurs easily. Corneal epithelial transplantation is one of the potential methods for corneal reconstruction after injury, but it requires the assistance of some form of scaffold. In this study, CMCTS or CMCT derived from the natural polymers chitin and chitosan were used for the preparation of epithelial scaffolds (Table 1). KAc was used as a porogen. In our previous studies, the presence of KAc resulted in the formation of holes in the

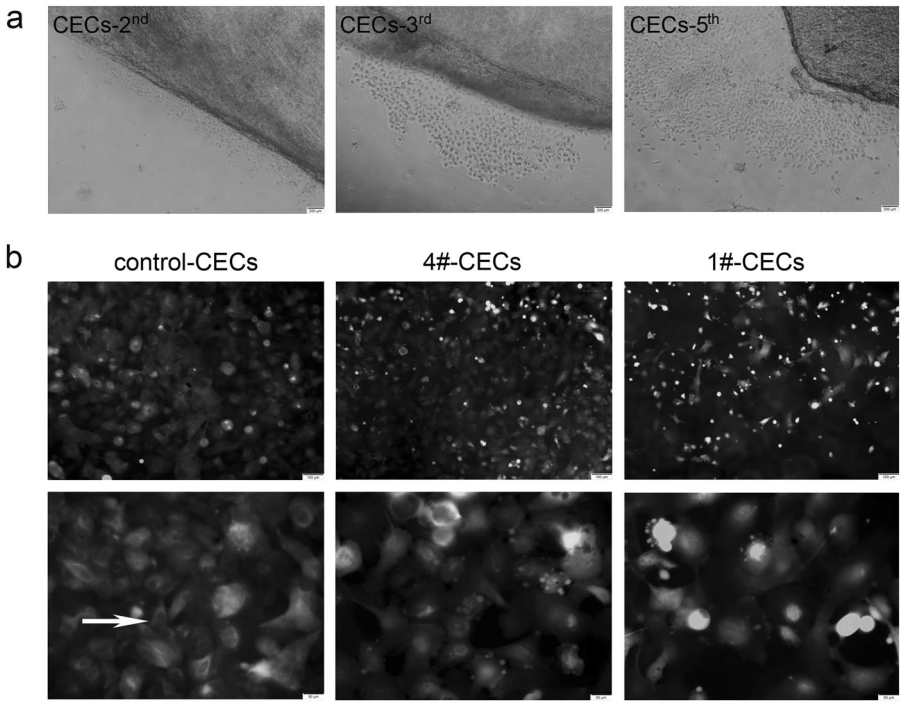

Fig. 4 Photomicrographs showing the primary CECs cultured by the tissue block method on the 2nd (CEC-2nd), 3rd (CEC-3rd), and 5th (CEC-5th) days (40×). The spread of CECs on the blend membranes based on CMCT (#4) (#4-CECs, 100×) and CMCTS (#1) (#1-CECs, 100×) after culturing for 48 h was observed by fluorescence microscopy. The corresponding amplification photos for #4 and #1 are #4-CECs and #1-CECs (200×), respectively. At the same time, CECs on glass slides were observed under afluorescence microscope at magnifications of 100× (control-CECs) and 200× (control-CECs) as a control

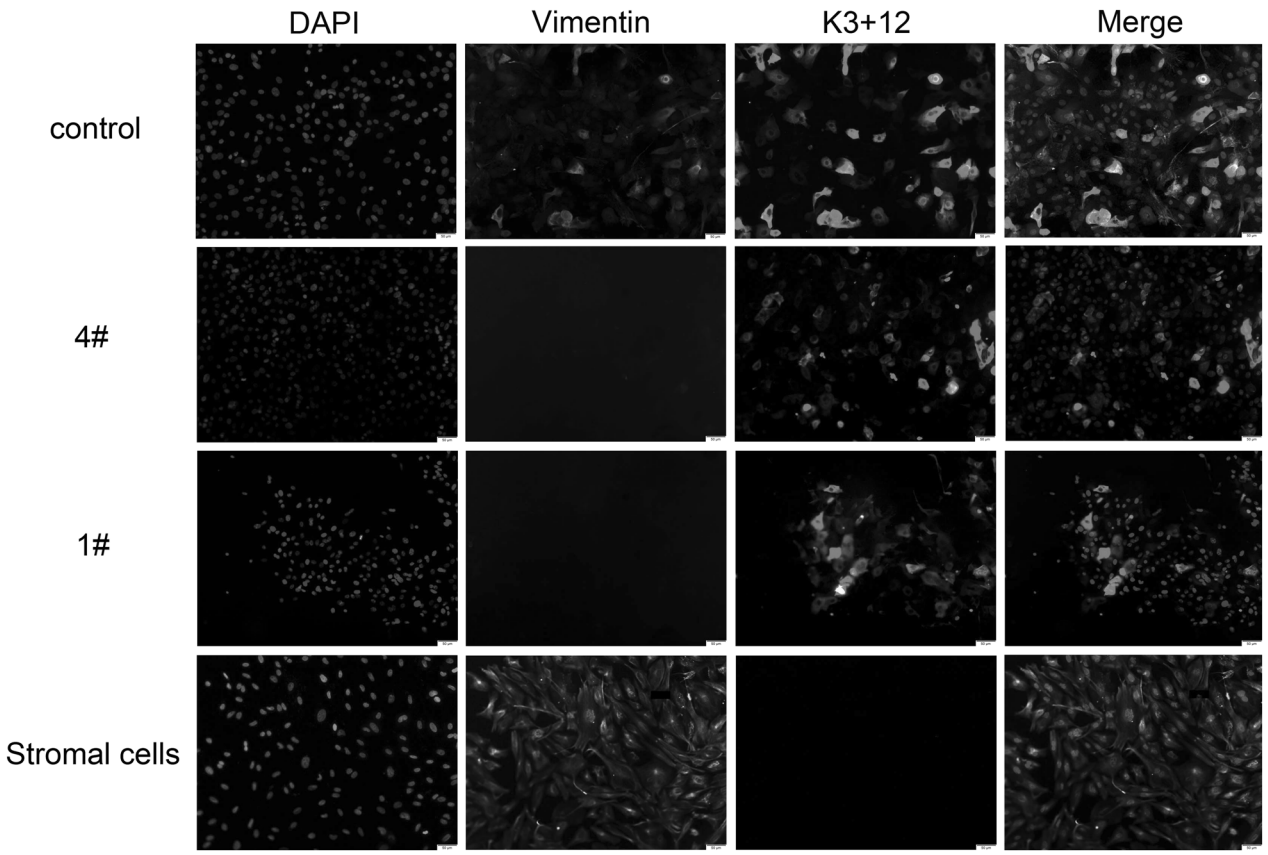

Fig. 5 Fluorescence images showing cell markers, including cytokeratin 3 + 12 (K3 + 12, red), vimentin (green) and cell nuclei (blue). CECs were cultured on glass slides as a control and on membranes #4 and #1 as experimental groups. Stromal cells were stained as a positive control for vimentin and a negative control for K3 + 12 (stromal cells) (200×)

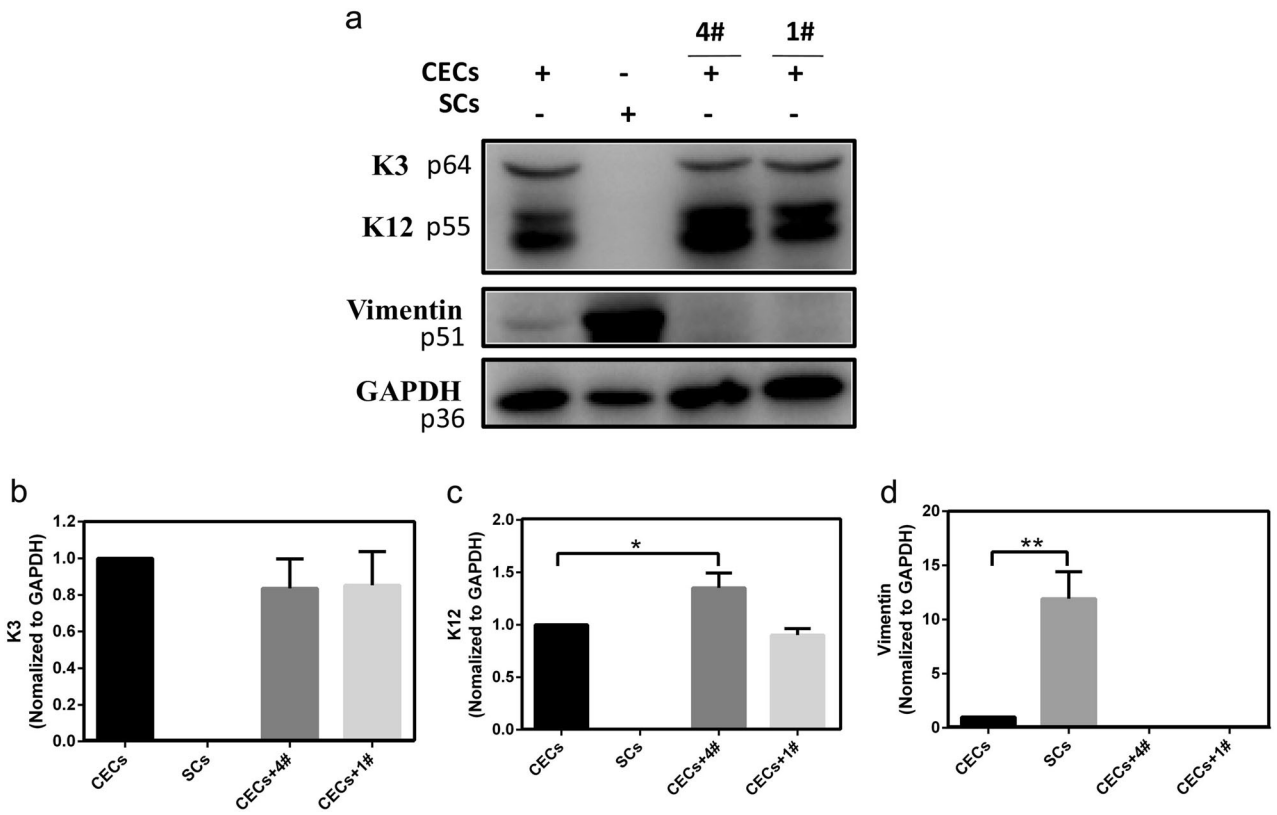

Fig. 6 Protein expression levels of K3 + 12 and vimentin were analyzed by a western blot assay (**a**). Quantification of K3 (**b**), K12 (**c**), and vimentin (**d**) protein levels, normalized by GAPDH. Data are presented as the mean ± SD for each group from three experiments. *$p < 0.05$: significantly different; **$p < 0.01$: highly significantly different

surface of membranes and promoted cell adhesion [25]. However, in this study, the materials containing different amounts of KAc, membranes #2, #3, #5, and #6, were not more suitable than membranes #1 and #4 for cell attachment (Fig. 3). Therefore, we confirmed that KAc could change the microstructure of blend membranes (Fig. 2) but that the added amount should be varied according to the characteristics of the materials and the degree of crosslinking.

A successful tissue engineering scaffold for the cornea is proposed to have certain characteristics, the most important of which is good cytocompatibility. We tested the properties of the blend membranes with different ratios of components, and the results demonstrated that HCE cells cultured on membranes #4 and #1 could maintain good activity and normal epithelial morphology (Fig. 3). However, this situation cannot completely reflect the real situation of primary corneal epithelial cells. Therefore, in further experiments, primary CECs were cultured on the blend membranes (Fig. 4), and the marker proteins of the CECs were studied by fluorescence microscopy (Fig. 5), which is of great value in the study of blend membranes used for tissue engineering. Basing on the microscopy results, there were more round cells on membrane #1, while the cells on membrane #4 could attach to each other and maintain the original epithelial morphology, which showed that membrane #4 might be more suitable for culturing CECs than membrane #1. However, according to the results of protein expression analysis, CECs cultured on both blend membranes maintained the expression of the epithelial marker protein K3 + 12 and did not express the fibrosis marker protein vimentin (Figs. 5, 6). In addition, the K12 protein level in the cells grown on membrane #4 was substantially improved. Based on these results, we explored the potential mechanism by which the membranes prevented fibrosis via related pathways in the subsequent studies.

Scarring in the cornea is characterized by the appearance of myofibroblasts. TGF-β has been confirmed as an important modulator of corneal myofibroblast development in vitro and in vivo and plays a critical role in wound healing via its pleiotropic effects on cell proliferation, differentiation and ECM accumulation [26]. The TGF-β signaling pathway is essential for modulating tissue growth as well as for wound healing after injury. However, TGF-β is arguably the most important ligand in the pathogenesis of fibrotic disease, and its overexpression in the cornea could lead to scarring [20]. In addition, the TGF-β/Smad signaling pathway is a classic route of TGF-β transduction. The effect of TGF-β can be mediated by serine/threonine kinase

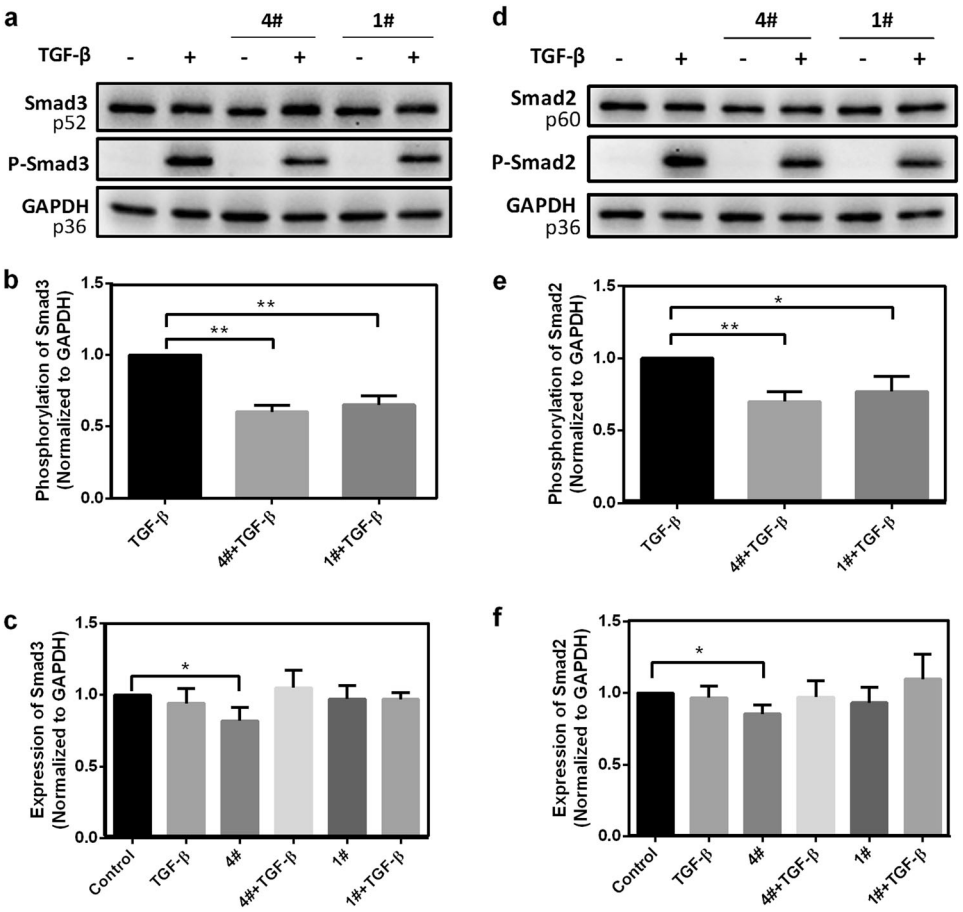

Fig. 7 Western blot analysis of phosphorylationand total Smad2 and Smad3 in HCE cellson CMCTS or CMCT blend membranes (**a**, **d**). Quantification of P-Smad3 (**b**), total Smad3 (**c**), P-Smad2 (**e**), and total Smad2 (**f**), normalized to GAPDH. Data are presented as the mean ± SD for each group from three experiments. $*p < 0.05$: significantly different; $**p < 0.01$: highly significantly different

receptor. When type I receptors are activated by TGF-β, Smad2 and Smad3 are phosphorylated to P-Smad2 and P-Smad3. Then, the activatedP-Smad2 and P-Smad3 combine with Smad4 to form oligomers and transfer to the nucleus to regulate gene expression. Research has shown that over activation of the TGF-β/Smad signaling path way could promote corneal fibrosis and result in scar formation [27]. Thus, inhibiting the over activation of the TGF-β/Smad path way could prevent corneal scarring.

Chitosan (CTS), the partially deacetylated form of chitin (CT), is a biocompatible polymerthat is widely distributed in the shells of crustaceans and the cytoderms of some fungi. CMCTS and CMCT can be slowly degraded to non-toxic monosaccharides in vivo, and can therefore function in the ECM by supporting cell adhesion and growth [28, 29]. Previous research [30] has studied the effects of CMCTS on normal and keloid skin fibroblasts and showed that CMCTS could promote the proliferation of normal skin fibroblasts and inhibit the proliferation of keloid fibroblasts. CMCTS inhibited the secretion of type I collagen, decreasing the collagen type I/III ratio in keloid fibroblasts, which has a close relationship with fibrosis inhibition. This study indicated that CMCTS can reduce fibrosis, which is consistent with our research. In addition, other studies have examined carboxymethyl chitosan as an ingredient in preparing a "phase change" anti-adhesion barrier for reducing peritoneal adhesion [31] and concluded that materials based on carboxymethyl chitosan can block fibrosis. Furthermore, N, O-carboxymethyl chitosan was shown to possess post-operative anti-adhesion ability in a rat model of cecal abrasion, reducing the expression of TGF-β_1 and exhibiting a positive inhibitory effect on fibrosis [32]. However, these studies were not based on the further anti-fibrosis regulation mechanisms of CMCTS but on cellular activity and cytokine secretion. Additional instances of the suppression of fibrosis by CTS have been reported [33, 34], although there have been few reports about chitin. CTS can improve tendon healing after surgery, which is reduced by the high expression of miR-29b and its down-regulation of the TGF-β1/Smad3 level and inhibition of fibroblast growth [32]. However, there have been no studies comparing the inhibitory effects of CMCT and CMCTS on fibrosis via the TGF-β1/Smads pathway. In addition, the inhibition of fibrosis by membranes based on CMCTS or CMCT has not been previously reported in corneal tissue engineering, and there were no clear reports on the specific mechanism of corneal fibrosis inhibition.

In our study, it was shown that the screened blend membranes could maintain the normal epithelial morphology and markers of CECs. Hence, taking TGF-β/Smad signaling as a starting point, experiments were conducted in vitro to investigate the underlying molecular mechanisms of the anti-fibrosis effects on corneal wound healing. The major finding of this study was that the phosphorylation levels of Smad2 and Smad3 induced by TGF-β were significantly decreased in epithelial cells cultured on CMCTS or CMCT membranes (#1 and #4). In addition, the total endogenous expression levels of Smad2 and Smad3 in the epithelial cells grown on membrane #4 were also significantly depressed. Therefore, the CMCT-based membrane inhibits fibrosis by regulating both the phosphorylation levels and the total endogenous levels of Smad2 and Smad3, and the application of this membrane in wound healing could play further positive roles in tissue engineering or medical therapeutics.

This study provides a novel engineering scaffold for corneal epithelial reconstruction. However, epithelial transplantation with these membranes in vivo also needs to be assessed in animal models in further studies.

Conclusion

In this study, two corneal epithelial carriers prepared with CMCTS (#1) or CMCT (#4) were successfully screened and showed good cytocompatibility. Both allow cells to maintain epithelial protein markers and prevent cell fibrosis. However, epithelial cells grown on membrane #4 maintain their original epithelial morphology and showed greatly improved K12 protein levels, and it was also proven that this blend membrane could block epithelial cell fibrosis by regulating both the endogenous levels and the phosphorylation and levels of the Smad2 and Smad3 proteins. This study provides a novel corneal epithelia scaffold that will be applied in corneal epithelial reconstruction based on tissue engineering methods.

Acknowledgements This study was financially supported by the National Natural Science Foundation of China (81770900), the Science and Technology Development Foundation of Shandong Province (2014GHY115025), the National Natural Science Foundations of China (81401899), the Qingdao Science and Technology Plan Fund (16-6-2-28-NSH), and the Qingdao Young Scientist Applied and Basic Research Fund (15-9-1-51-jch).

Compliance with ethical standards

Conflict of interest The authors declare that they have no conflict of interest.

References

1. Zhao K, Yang P. Ophthalmology. 8th ed. People's Medical Publishing House of China, Beijing, China, 2013.
2. Gautam S, Dinda AK, Mishra NC. Fabrication and characterization of PCL/gelatin composite nanofibrous scaffold for tissue engineering applications by electrospinning method. Mater Sci Eng C Mater Biol Appl. 2013;33:1228–35.
3. Aziz MA, Cabral JD, Brooks HJL, Moratti SC, Hanton LR. Antimicrobial Properties of a chitosan dextran-based hydrogel for surgical use. Antimicrob Agents Chemother. 2012;56:280–7.
4. Cabral JD, Roxburgh M, Shi Z, Liu LQ, McConnell M, Williams G, et al. Synthesis, physiochemical characterization, and biocompatibility of a chitosan/dextran-based hydrogel for post-surgical adhesion prevention. J Mater Sci Mater Med. 2014;25:2743–56.
5. Kong X, Xu W. Biodegradation and biocompatibility of a degradable chitosan vascular prosthesis. Int J Clin Exp Med. 2015;8:3498–505.
6. Zheng Z, Zhang W, Sun W, Li X, Duan J, Cui J, et al. Influence of the carboxymethyl chitosan anti-adhesion solution on the TGF-beta1 in a postoperative peritoneal adhesion rat. J Mater Sci Mater Med. 2013;24:2549–59.
7. Bhardwaj N, Nguyen QT, Chen AC, Kaplan DL, Sah RL, Kundu SC. Potential of 3-D tissue constructs engineered from bovine chondrocytes/silk fibroin-chitosan for in vitro cartilage tissue engineering. Biomaterials . 2011;32:5773–81.
8. Kim S, Bedigrew K, Guda T, Maloney WJ, Park S, Wenke JC, et al. Novel osteoinductive photo-cross-linkable chitosan-lactide-fibrinogen hydrogels enhance bone regeneration in critical size segmental bone defects. Acta Biomater. 2014;10:5021–33.
9. Meyer C, Stenberg L, Gonzalez-Perez F, Wrobel S, Ronchi G, Udina E, et al. Chitosan-film enhanced chitosan nerve guides for long-distance regeneration of peripheral nerves. Biomaterials . 2016;76:33–51.
10. Pok S, Myers JD, Madihally SV, Jacot JG. A multilayered scaffold of a chitosan and gelatin hydrogel supported by a PCL core for cardiac tissue engineering. Acta Biomater. 2013;9:5630–42.
11. Zakhem E, Raghavan S, Gilmont RR, Bitar KN. Chitosan-based scaffolds for the support of smooth muscle constructs in intestinal tissue engineering. Biomaterials . 2012;33:4810–7.
12. Bukzem AL, Signini R, dos Santos DM, Liao LM, Ascheri DPR. Optimization of carboxymethyl chitosan synthesis using response surface methodology and desirability function. Int J Biol Macromol. 2016;85:615–24.
13. Galli C, Parisi L, Elviri L, Bianchera A, Smerieri A, Lagonegro P, et al. Chitosan scaffold modified with D-(+) raffinose and enriched with thiol-modified gelatin for improved osteoblast adhesion. Biomed Mater. 2016;11:015004.
14. Jihui Wang ZW, Shangshang MA, Xizeng Feng. Synthesis, humidity controlling and antibacterial behaviors of potassium acetate/polyacrylamide composite. Chem Ind Eng Progress. 2009;26:189–93.
15. Tao Xu, W H, Jingzhong Cheng, Zheng Li, Gang Yu. Preparation and possible mechanism of potassium acetate/metakaolinite intercalated composites. Acta Petrol Et Mineral. 2009;28:670–4.
16. Chen Q, Lu H, Yang H. Chitosan inhibits fibroblasts growth in Achilles tendon via TGF-beta1/Smad3 pathway by miR-29b. Int J Clin Exp Pathol. 2014;7:8462–70.
17. Lauder CIW, Strickland A, Maddern GJ. Use of a modified chitosan-dextran gel to prevent peritoneal adhesions in a porcine hemicolectomy model. J Surg Res. 2012;176:448–54.
18. Sun Y, Yan LQ, Liang Y, Li XL, Cao XJ, Lu C. Reduction of epidural scar adhesion by topical application of simvastatin after laminectomy in rats. Eur Rev Med Pharmacol Sci. 2015;19:3–8.

19. Wu W, Lee SY, Wu XB, Tyler JY, Wang H, Ouyang Z, et al. Neuroprotective ferulic acid (FA)-glycol chitosan (GC) nanoparticles for functional restoration of traumatically injured spinal cord. Biomaterials . 2014;35:2355–64.
20. Tandon A, Tovey JC, Sharma A, Gupta R, Mohan RR. Role of transforming growth factor Beta in corneal function, biology and pathology. Curr Mol Med. 2010;10:565–78.
21. Ljubimov AV, Saghizadeh M. Progress in corneal wound healing. Prog Retin Eye Res. 2015;49:17–45.
22. Chen XG, Park HJ. Chemical characteristics of O-carboxymethyl chitosans related to the preparation conditions. Carbohydr Polym. 2003;53:355–9.
23. Wongpanit P, Sanchavanakit N, Pavasant P, Supaphol P, Tokura S, Rujiravanit R. Preparation and characterization of microwave-treated carboxymethyl chitin and carboxymethyl chitosan films for potential use in wound care application. Macromol Biosci. 2005;5:1001–12.
24. Liang Y, Xu W, Han B, Li N, Zhao W, Liu W. Tissue-engineered membrane based on chitosan for repair of mechanically damaged corneal epithelium. J Mater Sci Mater Med. 2014;25:2163–71.
25. Liang Y, Liu W, Han B, Yang C, Ma Q, Zhao W, et al. Fabrication and characters of a corneal endothelial cells scaffold based on chitosan. J Mater Sci Mater Med. 2011;22:175–83.
26. Finnson KW, McLean S, Di Guglielmo GM, Philip A. Dynamics of transforming growth factor beta signaling in wound healing and scarring. Adv Wound Care. 2013;2:195–214.
27. Sumioka T, Ikeda K, Okada Y, Yamanaka O, Kitano A, Saika S. Inhibitory effect of blocking TGF-beta/Smad signal on injury-induced fibrosis of corneal endothelium. Mol Vis. 2008;14:2272–81.
28. Chang J, Liu W, Han B, Peng S, He B, Gu Z. Investigation of the skin repair and healing mechanism of *N*-carboxymethyl chitosan in second-degree burn wounds. Wound Repair Regen. 2013;21:113–21.
29. Wang D, Mo J, Pan S, Chen H, Zhen H. Prevention of post-operative peritoneal adhesions by O-carboxymethyl chitosan in a rat cecal abrasion model. Clin Invest Med. 2010;33:E254–60.
30. Chen XG, Wang Z, Liu WS, Park HJ. The effect of carboxymethyl-chitosan on proliferation and collagen secretion of normal and keloid skin fibroblasts. Biomaterials . 2002;23:4609–14.
31. Li XD, Xia DL, Shen LL, He H, Chen C, Wang YF, et al. Effect of “phase change” complex on postoperative adhesion prevention. J Surg Res. 2016;202:216–24.
32. Zhu L, Zhang YQ. Postoperative anti-adhesion ability of a novel carboxymethyl chitosan from silkworm pupa in a rat cecal abrasion model. Mater Sci Eng C Mater Biol Appl. 2016;61:387–95.
33. Mandapalli PK, Labala S, Jose A, Bhatnagar S, Janupally R, Sriram D, et al. Layer-by-layer thin films for co-delivery of TGF-beta siRNA and epidermal growth factor to improve excisional wound healing. AAPS PharmSciTech. 2017;18:809–20.
34. Rajabian MH, Ghorabi GH, Geramizadeh B, Sameni S, Ayatollahi M. Evaluation of bone marrow derived mesenchymal stem cells for full-thickness wound healing in comparison to tissue engineered chitosan scaffold in rabbit. Tissue Cell. 2017;49:112–21.